Journal of Ginseng Research 47 (2023) 408–419

Contents lists available at ScienceDirect

Journal of Ginseng Research

journal homepage: https://www.sciencedirect.com/journal/journal-of-ginseng-research

Research Article

Ginsenoside compound K protects against cerebral ischemia/reperfusion injury via Mul1/Mfn2-mediated mitochondrial dynamics and bioenergy

Qingxia Huang [a, b], Jing Li [b], Jinjin Chen [b], Zepeng Zhang [a, b], Peng Xu [c], Hongyu Qi [b], Zhaoqiang Chen [b], Jiaqi Liu [b], Jing Lu [a, c], Mengqi Shi [d], Yibin Zhang [c], Ying Ma [c], Daqing Zhao [b], Xiangyan Li [b, *]

[a] Research Center of Traditional Chinese Medicine, College of Traditional Chinese Medicine, Changchun University of Chinese Medicine, Changchun, Jilin, China
[b] Northeast Asia Research Institute of Traditional Chinese Medicine, Key Laboratory of Active Substances and Biological Mechanisms of Ginseng Efficacy, Ministry of Education, Jilin Provincial Key Laboratory of Bio-Macromolecules of Chinese Medicine, Changchun University of Chinese Medicine, Changchun, Jilin, China
[c] Department of Encephalopathy, College of Traditional Chinese Medicine, Changchun University of Chinese Medicine, Changchun, Jilin, China
[d] Department of Graduate Administration, College of Traditional Chinese Medicine, Changchun University of Chinese Medicine, Changchun, Jilin, China

ARTICLE INFO

Article history:
Received 6 June 2022
Received in revised form
15 September 2022
Accepted 11 October 2022
Available online 20 October 2022

Keywords:
Ginsenoside compound K
Cerebral ischemia/reperfusion injury
Mitochondrial dynamics
Bioenergy
Mul1/Mfn2 ubiquitination

ABSTRACT

Background: Ginsenoside compound K (CK), the main active metabolite in *Panax ginseng*, has shown good safety and bioavailability in clinical trials and exerts neuroprotective effects in cerebral ischemic stroke. However, its potential role in the prevention of cerebral ischemia/reperfusion (I/R) injury remains unclear. Our study aimed to investigate the molecular mechanism of ginsenoside CK against cerebral I/R injury.

Methods: We used a combination of *in vitro* and *in vivo* models, including oxygen and glucose deprivation/reperfusion induced PC12 cell model and middle cerebral artery occlusion/reperfusion induced rat model, to mimic I/R injury. Intracellular oxygen consumption and extracellular acidification rate were analyzed by Seahorse multifunctional energy metabolism system; ATP production was detected by luciferase method. The number and size of mitochondria were analyzed by transmission electron microscopy and MitoTracker probe combined with confocal laser microscopy. The potential mechanisms of ginsenoside CK on mitochondrial dynamics and bioenergy were evaluated by RNA interference, pharmacological antagonism combined with co-immunoprecipitation analysis and phenotypic analysis.

Results: Ginsenoside CK pretreatment could attenuate mitochondrial translocation of DRP1, mitophagy, mitochondrial apoptosis, and neuronal bioenergy imbalance against cerebral I/R injury in both *in vitro* and *in vivo* models. Our data also confirmed that ginsenoside CK administration could reduce the binding affinity of Mul1 and Mfn2 to inhibit the ubiquitination and degradation of Mfn2, thereby elevating the protein level of Mfn2 in cerebral I/R injury.

Conclusion: These data provide evidence that ginsenoside CK may be a promising therapeutic agent against cerebral I/R injury via Mul1/Mfn2–mediated mitochondrial dynamics and bioenergy.

© 2022 The Korean Society of Ginseng. Publishing services by Elsevier B.V. This is an open access article under the CC BY-NC-ND license (http://creativecommons.org/licenses/by-nc-nd/4.0/).

1. Introduction

Cerebral ischemia/reperfusion (I/R) injury is a pathological condition that may occur with the recovery of blood circulation in the treatment of ischemic stroke, which eventually leads to acute neurological deficit [1]. A growing body of preclinical and clinical evidence indicates that mitochondria, as dynamic organelles

* Corresponding author. Jilin Ginseng Academy, Key Laboratory of Active Substances and Biological Mechanisms of Ginseng Efficacy, Ministry of Education, Jilin Provincial Key Laboratory of BioMacromolecules of Chinese Medicine, Changchun University of Chinese Medicine, Changchun, Jilin, 130117, China.
E-mail addresses: zhaodaqing1963@163.com (D. Zhao), xiangyan_li1981@163.com (X. Li).

https://doi.org/10.1016/j.jgr.2022.10.004
1226-8453/© 2022 The Korean Society of Ginseng. Publishing services by Elsevier B.V. This is an open access article under the CC BY-NC-ND license (http://creativecommons.org/licenses/by-nc-nd/4.0/).

manage to retain the balance of fusion/fission dynamics in neuronal I/R situations [2]. Mitochondrial fusion accelerates the exchange of nutrition materials and assists in the repair of damaged mitochondria, while mitochondrial fission is an important step in the removal of defective mitochondria through mitophagy [3,4]. During I/R injury, the superoxide production by complex I reverse electron transport (RET) results in stunted mitochondrial fusion and fission, which in conjunction with traumatic mitophagy leads to dysfunctions of the Krebs cycle and oxidative phosphorylation (OXPHOS) [5]. Abnormal mitochondrial bioenergy leads to reduced mitochondrial respiration function and neuronal injury [6]. Hence, regulation of dynamics (elevated fusion and suppressed fission) and bioenergy promotion of mitochondria may play neuroprotective effects against cerebral I/R induced injury.

Mitochondrial E3 ubiquitin ligase 1 (Mul1) is a multifunctional mitochondrial membrane protein and acts as the first-line surveillance of mitochondrial dynamics and energy supply in neuronal I/R injury [7,8]. In neurons, mitochondrial dynamic fusion is mainly controlled by optic atrophy protein 1 (OPA1) and mitofusins (Mfn1 and Mfn2), while fission depends on dynamin–related protein 1 (DRP1) and fission 1 protein (FIS1) [9,10]. In mammalian systems, the E3-active, C-terminal RING finger domain of Mul1 faces the cytosol, which can stabilize DRP1 and degrade mitofusins through ubiquitin-like modifiers and ubiquitination [11,12]. As expected from Mul1 protein with these proposed biochemical activities, I/R–induced Mul1 overexpression in neurons results in smaller and more fragmented mitochondria, enhanced mitophagy, inhibited OXPHOS, imbalance in energy homeostasis, and mitochondrial apoptosis [13]. Thus, the suppression of Mul1 activity and expression can regulate mitochondrial dynamics and mitophagy to enhance mitochondrial bioenergy against I/R damage in neurons.

Ginsenoside compound K (CK), one of the main active metabolites from traditional Chinese medicine, *Panax ginseng*, has shown good safety and bioavailability in clinical trials, and exerts neuroprotective effects in neurodegenerative diseases and cerebral ischemic stroke [14–17]. It has been shown that ginsenoside CK reduces the infarct volume of the cerebral I/R model induced by middle cerebral artery occlusion (MCAO) and suppresses microglial activation in the mice ischemic cortex [18]. Our previous studies have demonstrated that ginsenoside CK inhibits reactive oxygen species (ROS) burst and autophagy–mediated apoptosis, thereby acting against I/R injury [15]. Our literature review has found that ginsenoside CK can target mitochondrial ROS and function to inhibit metabolic stress [19]. Importantly, our latest *in vivo* and *in vitro* studies have shown that ginsenoside Rc, a key metabolic precursor of ginsenoside CK, can inhibit brain I/R injury by increasing mitochondrial biosynthesis and ATP production, and inhibiting mitochondrial apoptosis [20]. These studies have indicated that ginsenoside CK can significantly reduce cerebral I/R injury, and its effect may be related to mitochondrial function and energy metabolism. However, the underlying protective mechanism by which ginsenoside CK regulates mitochondrial function and bioenergy production against I/R damage remains to be elucidated. Hence, the present study was designed to investigate the pharmacological mechanism of ginsenoside CK against cerebral I/R induced injury based on Mul1/Mfn2–mediated mitochondrial dynamics and bioenergy in *in vitro* and *in vivo* studies.

2. Materials and methods

2.1. Antibodies and reagents

Oligomycin B (ab143424), antimycin A (ab141904), and antibodies against total OXPHOS (ab110413), Mfn1 (ab104274), Mfn2 (ab56889), DRP1 (ab56788), ubiquitin (Abcam, ab140601), FIS1 (ab71498), and OPA1 (ab90857) were obtained from Abcam (Cambridge, MA, USA). Antibodies to TOM20 (#42406), LC3A/B (#4108), P-DRP1 (Ser637, #4867), and β-Actin (#3700) were purchased from Cell Signaling Technology (Beverly, MA, USA). Mul1 (16133-1-AP) and Parkin (14060-1-AP) antibodies were purchased from Proteintech (Wuhan, Hubei, China). Carbonyl cyanide 4-(trifluoromethoxy) phenylhydrazone (FCCP, C2920), rotenone (R8875), and Mdivi-1 (M0199) were purchased from Sigma-Aldrich (St. Louis, MO, USA). Ginsenoside CK was purchased from Yuanye Bio-Technology (HPLC $\geq$ 98%, Shanghai, China).

2.2. siRNA transfection

Predesigned siRNAs for rat Mul1 (siG150514163245-1-5) and Mfn2 (siG141230171112-1-5) and negative control siRNA (siB160812022401-1-5) were provided by RiboBio (Guangzhou, China) and transfected into PC12 cells using Lipofectamine RNAiMAX (Invitrogen). Briefly, the diluted siRNA and transfection reagent in Opti-MEM (Invitrogen) were incubated for 5 min at room temperature to allow for the formation of siRNA-lipid complexes. After washing twice by Opti-MEM, the cells were incubated with the siRNA–lipid complexes for 48 h. We examined the efficiency of siRNA silencing by western blot and then subjected the cells to various treatments as planned [21].

2.3. Co-immunoprecipitation (co-IP) analysis

Proteins from PC12 cells and brain tissues were extracted in NP-40 lysis buffer (Beyotime) containing a complete protease inhibitor cocktail (Sigma-Aldrich) [22]. The protein extracts were subjected to centrifugation at 12,000g for 12 min. After the specified antibodies were bound to protein lysate at 4°C overnight, the antigen–antibody complexes were immunoprecipitated with the A/G magnetic beads at room temperature for 1 h. After separating the beads with a magnetic rack, the pellets were eluted with sample buffer and boiled at 100 °C for 5 min. The magnetic beads were separated, and the supernatant was loaded onto an acrylamide gel.

2.4. Seahorse analysis

To investigate the ATP production from OXPHOS and glycolysis, oxygen consumption rate (OCR) and extracellular acidification rate (ECAR) were determined using the Seahorse XFe24 analyzer (Seahorse Bioscience, Billerica, MA, USA) as reported previously [20]. Briefly, the cells were plated in a Seahorse XFe24 cell culture plate before pretreatment with ginsenoside CK and/or OGD/R incubation. The medium was then exchanged with Seahorse XF DMEM medium (Seahorse Bioscience) containing 2 mM glutaMAX (Invitrogen), 1 mM sodium pyruvate (Invitrogen), and 10 mM glucose, which were equilibrated for 30 min at 37°C before the experiment. Cellular ATP, OCR, or ECAR was monitored in basal conditions (before any addition) and after the addition of glucose (Glu), oligomycin (Olig), 2-D-glucose (2-DG), FCCP or rotenone (Rot) & antimycin A (AA) with three cycles of mixing (150 s), waiting (120 s) and measuring (210 s). The ATP, OCR, or ECAR values were normalized to cell numbers in the corresponding wells and expressed as pmol/min/10^4 cells or mpH/min/10^4 cells.

2.5. Transmission electron microscopy (TEM)

After pretreatment with ginsenoside CK and/or I/R injury, the brains were cut into 2-mm sections and fixed in ice-cold 2.5% glutaraldehyde solution for 15 min. Then, the tissue sections were postfixed in 0.7% potassium ferrocyanide, stained with 2.5% uranyl

acetate in 0.1 M maleate, and embedded in Eponate (TedPella, CA, USA). The tissue sections were polymerized overnight and immersed in liquid nitrogen. Thin sections with 60–80 nm were cut with a diamond knife on a Leica EM UC7 ultramicrotome with ultra 45° (Daitome) and collected onto copper grids, which were stained with 4% uranyl acetate in 50% methanol and 5% citrate [23]. Images were captured with a transmission electron microscope (TECNAI G2 20 TWIN, FEI, Hillsboro, OR, USA).

2.6. Data and statistical analysis

All the *in vivo* and *in vitro* experimental groups were designed to establish equal size, blinding, and randomization [24]. All group sizes represent the numbers of experimental independent values; these independent values were used for statistical analyses, and statistical analyses were undertaken only for experiments where each group size (n) was ≥ 3. Values are expressed as mean ± SD in *in vitro* study and mean ± SEM in *in vivo* study. The normality test (D'Agostino–Pearson) and equal variance test (Brown–Forsythe) were applied. The two-tailed Student's *t* test was used for comparison between the two groups. Multigroup comparisons were performed using the one-way ANOVA followed by Tukey's post-hoc test. The post hoc tests were conducted only if the F value in ANOVA achieved the necessary statistical significance level and there was no significant variance inhomogeneity. The analyses were performed in GraphPad Prism 8.0. $P < 0.05$ was considered statistically significant [25].

Supporting information

Details of materials preparation and full experimental procedures, including cell culture and oxygen–glucose deprived/reperfusion (OGD/R) model, Animals and middle cerebral artery occlusion model, quantification of mitochondrial DNA content, mitochondria isolation, mitochondrial and mitophagy morphology, Western blot, immunofluorescence staining, ATP production assay, measurement of mitochondrial complex I–V activity, measurement of the mitochondrial membrane potential and reactive oxygen species, TTC staining, neurological deficit score, H&E staining, Nissl staining, and immunohistochemistry analysis are given in the Supplementary Information.

3. Results

3.1. Ginsenoside CK rescues OGD/R-induced mitochondrial dysfunction in a manner dependent on Mfn2 inactivation

We analyzed whether ginsenoside CK regulates Mfn2 to restore mitochondrial function. First, the dose-dependent effect of ginsenoside CK on ATP content was evaluated by a luminescence assay. Multigroup studies comparisons were performed using the One-way ANOVA followed by a Tukey's post hoc test. $P < 0.05$ was considered statistically significant. Our results showed that ginsenoside CK at the concertation of 2, 4, and 8 μM significantly restored the decrease in ATP synthesis caused by OGD/R(Fig. S1A). We also found that ginsenoside CK increased the ATP content mainly from mitochondria, and had no obvious effect on ATP production from glycolysis (Fig. 1A). To further verify the origin of increased ATP mediated by ginsenoside CK, OCR was monitored in real-time to measure the key parameters of mitochondrial function by adding different modulators of respiration. As expected, we found that ginsenoside CK caused an enhancement in respiratory capacity, but had no significant effect on ECAR in the OGD/R-induced injury (Fig. 1B and C). To evaluate the effect of ginsenoside CK on the electron transport chain (ETC), we examined the expression levels and activities of the mitochondrial complex I–V, and the copy number of mitochondrial DNA. As shown in Fig. 1D-F and Fig. S1B, ginsenoside CK had no obvious effect on the expression of complex I–V and the ratio of mitochondrial DNA/nuclear DNA compared with the OGD/R group, but it had a significant promotion effect on the activities of mitochondrial complex I (NADH-CoQ reductase) and III (CoQ-Cytochrome C reductase). Importantly, we found that the effect of ginsenoside CK pretreatment in promoting mitochondrial oxygen consumption in OGD/R-injured PC12 cells was completely abolished by Mfn2 knockdown (Fig. 1G and Fig. S1C), compared with the si-Ctrl group. These results suggest that ginsenoside CK rescues OGD/R-induced mitochondrial dysfunction, which might be dependent on Mfn2 signaling.

3.2. Ginsenoside CK balance mitochondria dynamics and mitophagy in OGD/R-induced PC12 model in an Mfn2-dependent manner

We further evaluated the effect of ginsenoside CK on mitochondrial dynamics and mitophagy in OGD/R injury and whether it is Mfn2-dependent. As shown in Fig. S2A–Fig. S2B, ginsenoside CK incubation decreased mitochondrial fragmentation in a dose-dependent manner, compared with the OGD/R group. Consistent with the expectations, knockdown of Mfn2 blocked the inhibitory effect of ginsenoside CK on mitochondrial fission in OGD/R-injured PC12 cells (Fig. 2A). The p62 protein interacts with LC3II, which is degraded in the autolysosomes. Immunoblot analysis showed that ginsenoside CK pretreatment increased the level of p62 and decreased the ratio of LC3II/LC3I in OGD/R injury (Fig. 2B). In addition, we observed that the autolysosomes (mCherry-positive/GFP-positive; yellow dots) decreased significantly after ginsenoside CK administration prior to OGD/R incubation (Fig. 2C and Fig. S2C), confirming the effect of ginsenoside CK in reducing autophagy. To determine whether Mfn2-regulated mitophagy contributes to neuroprotection of ginsenoside CK against OGD/R injury, Parkin translocation to mitochondria, and co-localization of mitochondria and lysosomes were evaluated in si-Ctrl or si-Mfn2 transfected cells. The translocation of Parkin to mitochondria significantly induced by OGD/R was reversed by ginsenoside CK, while Mfn2 knockdown markedly abrogated the mitigation effect of ginsenoside CK in terms of mitophagy (Fig. 2D and Fig. S2D). Similarly, Mfn2 knockdown counteracted the effect of ginsenoside CK in reducing the co-localization of mitochondria and lysosomes (Fig. 2E and Fig. S2E). These results indicate that the effects of ginsenoside CK on mitochondrial dynamics and mitophagy are mediated by the Mfn2 signaling in the OGD/R-induced PC12 cell model.

3.3. Ginsenoside CK inhibits OGD/R-induced neuronal injury by regulating the Mul1/Mfn2 pathway

To further clarify the regulatory effect of ginsenoside CK on Mul1 and mitochondrial dynamics–related signaling pathways during OGD/R injury, we separated cytoplasmic and mitochondrial proteins of PC12 cells untreated or treated with ginsenoside CK for western blot analysis. OGD/R incubation caused the decreased DRP1 phosphorylation at S637 and the slightly increased DRP1 in the cytoplasmic and mitochondrial proteins (Fig. 3A and Fig. S3A). Meanwhile, we observed that OGD/R incubation also resulted in the significant decreases in mitochondrial fusion–related proteins and the obvious increases in Mul1 and mitochondrial fission–related proteins (Fig. 3A and Fig. S3A). Importantly, our results showed that ginsenoside CK pretreatment prior to OGD/R incubation significantly reduced the expression of Mul1 and the translocation of DRP1 to mitochondria, and increased Mfn2 expression in

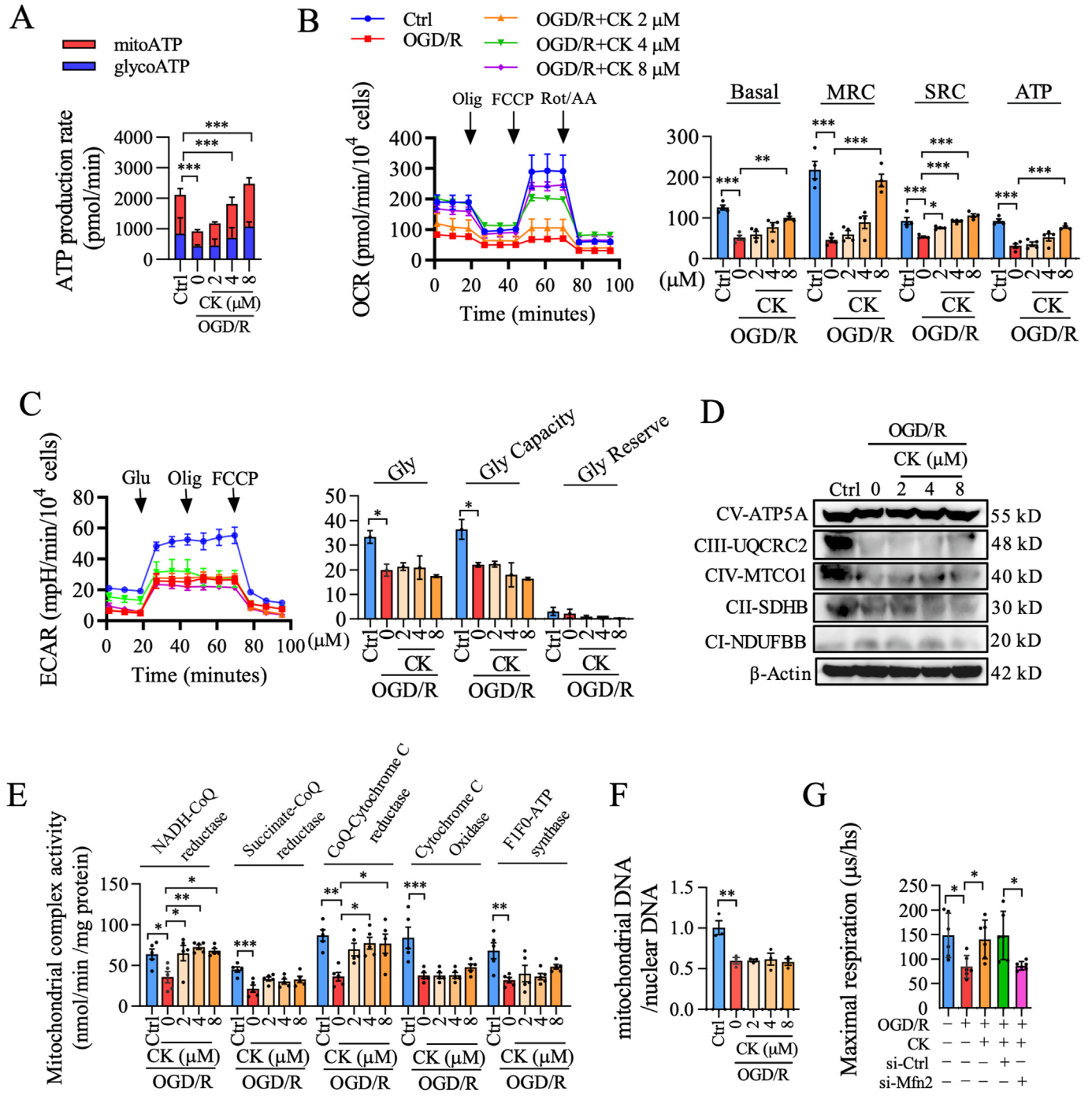

Fig. 1. The effect of ginsenoside CK against neuronal bioenergy imbalance is driven by Mfn2 inactivation in the OGD/R injury model. **(A)** The PC12 cells were treated with oligomycin (Olig) or rotenone plus antimycin A to detect the ATP production originated from the mitochondria (mitoATP) or glycolysis (glycoATP). **(B)** Oxygen consumption was measured and analyzed by Seahorse XFe24 multifunctional energy metabolizer and mitochondrial pressure kit; the relative levels of oxygen consumption for basal respiration (Basal), maximal respiration consumption (MRC), spare capacity (SPC), and ATP-linked respiration (ATP) are shown on the right. **(C)** Glycolysis (Gly), glycolytic capacity (Gly Capacity), and glycolytic reserve (Gly Reserve) were determined by the sequential addition of 10 mM glucose (Glu), 1 μM oligomycin (Olig), or 50 mM 2-deoxy-D-glucose (2-DG) by measuring extracellular acidification rate (ECAR). **(D)**The expression of mitochondrial complex protein I–V was detected by western blot. β-Actin was a loading control. **(E)** The activities of five mitochondrial electron transfer chain enzymes were determined by enzymatic reaction kinetics kit. **(F)** The ratio of mitochondrial DNA/nuclear DNA was evaluated by qPCR. **(G)** The maximal oxygen consumption was analyzed by the LUXCEL oxygen consumption probe in the PC12 cells. Data are shown as mean ± SD, n = 3 per group; *P < 0.05, **P < 0.01 and ***P < 0.001, significantly different as indicated (one-way ANOVA followed by Tukey's post hoc test).

mitochondria (Fig. 3A and Fig. S3A). Since Mul1 mainly regulates mitochondrial dynamics through ubiquitination of Mfn2, we then conducted a co-IP experiment to verify the regulatory effect of ginsenoside CK on the Mul1/Mfn2 signaling pathway. As expected, when Mul1 was immunoprecipitated, the protein binding of Mfn2 with Mul1 was significantly reduced after ginsenoside CK treatment, which means that ginsenoside CK reduced the degradation of Mfn2 by Mul1 after OGD/R incubation (Fig. 3B). In contrast, after Mfn2 was immunoprecipitated, OGD/R-induced Mul1 expression and the level of ubiquitination were obviously reduced by

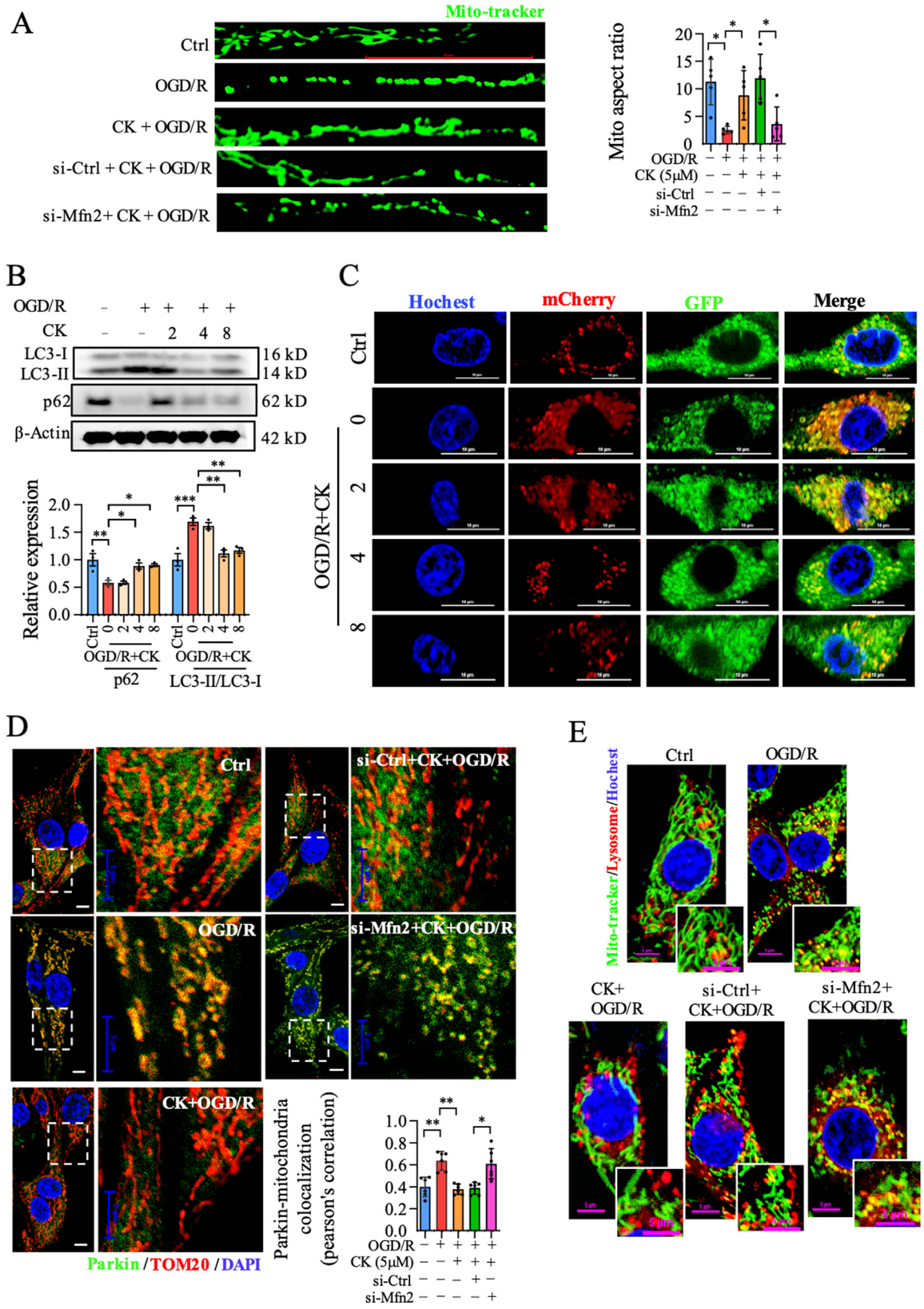

Fig. 2. Ginsenoside CK augments mitochondrial fusion and inhibits mitophagy through Mfn2 in the OGD/R-induced PC12 injury model. (A) After labeling with a Mito-tracker probe, mitochondrial morphology was visualized to analyze mitochondria aspect ratio; scale bar = 20 μm. **(B)** The expression of LC3-II / LC3-II and p62 was detected by western blot. **(C)** Analysis of the co-location of the GFP-RFP-LC3 fusion protein by confocal microscope; Hochest 33254 was used for nuclear staining; scale bar = 10 μm. **(D)** The co-localization of Parkin and TOM20 was detected and analyzed; DAPI was used for staining nucleus. Scale bar = 5 μm. **(E)** The co-location of mitochondria and lysosomes was visualized by confocal microscope; Hochest 33254 was used for nuclear staining; scale bar = 5 μm. Data are shown as mean ± SD, n = 3 per group; *P < 0.05, significantly different as indicated (one-way ANOVA followed by Tukey's post hoc test).

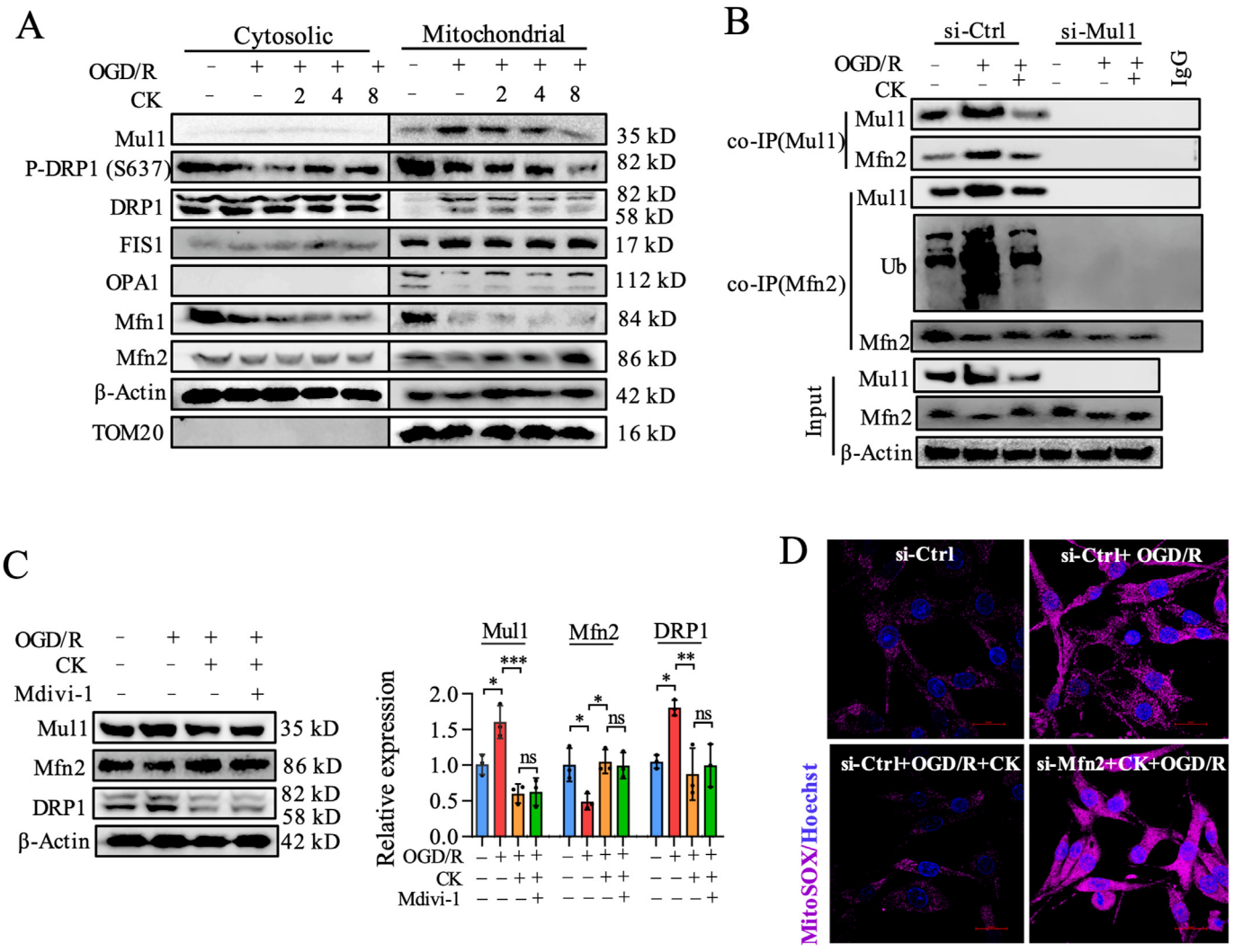

Fig. 3. Ginsenoside CK inhibits mitochondrial dynamics imbalance and damage by inhibiting the ubiquitination of Mfn2 by Mul1. **(A)** The expression of Mul1 and mitochondrial dynamics-related proteins in cytoplasm or mitochondria was detected by western blot; β-Actin and TOM20 were the loading controls for cytosolic and mitochondrial proteins, respectively. **(B)** After Mul1 or Mfn2 was immunoprecipitated, the binding and ubiquitination level of Mfn2 in mitochondrial proteins were detected by western blot analysis; 10% of the lysed mitochondrial proteins in the co-IP experiment were used as input control. **(C)** The expression of Mul1, Mfn2, and DRP1 were detected by western blot and quantitatively analyzed by ImageJ software. **(D)** The level of mitochondrial ROS (MitoSox) was determined by confocal microscope; scale bar = 20 μm. Hochest 33254 was used as a nuclear counterstain.

ginsenoside CK, which suggests that ginsenoside CK pretreatment did reduce Mul1-mediated Mfn2 ubiquitination and degradation during the OGD/R injury (Fig. 3B).

To identify whether the contribution of ginsenoside CK firstly regulates the binding of Mul1 and Mfn2, and then influences mitochondrial fission, mitophagy, and mitochondrial apoptosis, Mdivi-1, a widely used inhibitor of mitochondrial fission, was introduced to investigate the mechanism of ginsenoside CK in OGD/R-induced injury. In combination with Mdivi-1 treatment at 10 μM for 24 h, the effect of ginsenoside CK on reducing Mul1 expression and increasing Mfn2 expression was preserved, which means that mitochondrial fission occurred after the Mul1/Mfn2 signaling pathway (Fig. 3C). In addition, Mfn2 knockdown reversed ginsenoside CK–related inhibition of the production of mitochondrial ROS to prevent OGD/R injury (mito-ROS, Fig. 3D and Fig. S3B). These results suggest that ginsenoside CK mainly regulates Mul1 to reduce the ubiquitination and degradation of Mfn2, resulting in increased Mfn2 expression to inhibit mitochondrial fission, mitophagy, and mitochondrial apoptosis in OGD/R neuronal injury.

3.4. Ginsenoside CK counteracts I/R-induced neurological impairment and mitochondrial dysfunction in rats

To investigate the therapeutic effect of ginsenoside CK on cerebral I/R injury, we evaluated the infarct volume, neurological deficit score, and brain water content in the rat model. TTC staining showed that the infarct volume of the ginsenoside CK pretreatment group was significantly smaller than that of the I/R group (Fig. 4A and B). After ginsenoside CK pretreatment, the neurological function score decreased significantly after 24 h, compared with the I/R group (Fig. 4C). Moreover, ginsenoside CK pretreatment relieved cerebral edema caused by I/R injury (Fig. 4D). In addition, H&E and Nissl staining showed that the neurons in the cortex, CA1, CA3, striatum, and gyrus in rats with cerebral I/R injury were arranged loosely, and exhibited cell body shrinkage, partial nuclear fragmentation, nuclear pyknosis, nucleolar blurring, and even degeneration (Fig. 4E and Fig. S4A-S4B). Compared with the I/R injury group, ginsenoside CK administration significantly restored the damage to neurons in the cerebral cortex and CA1 regions (Fig. 4E).

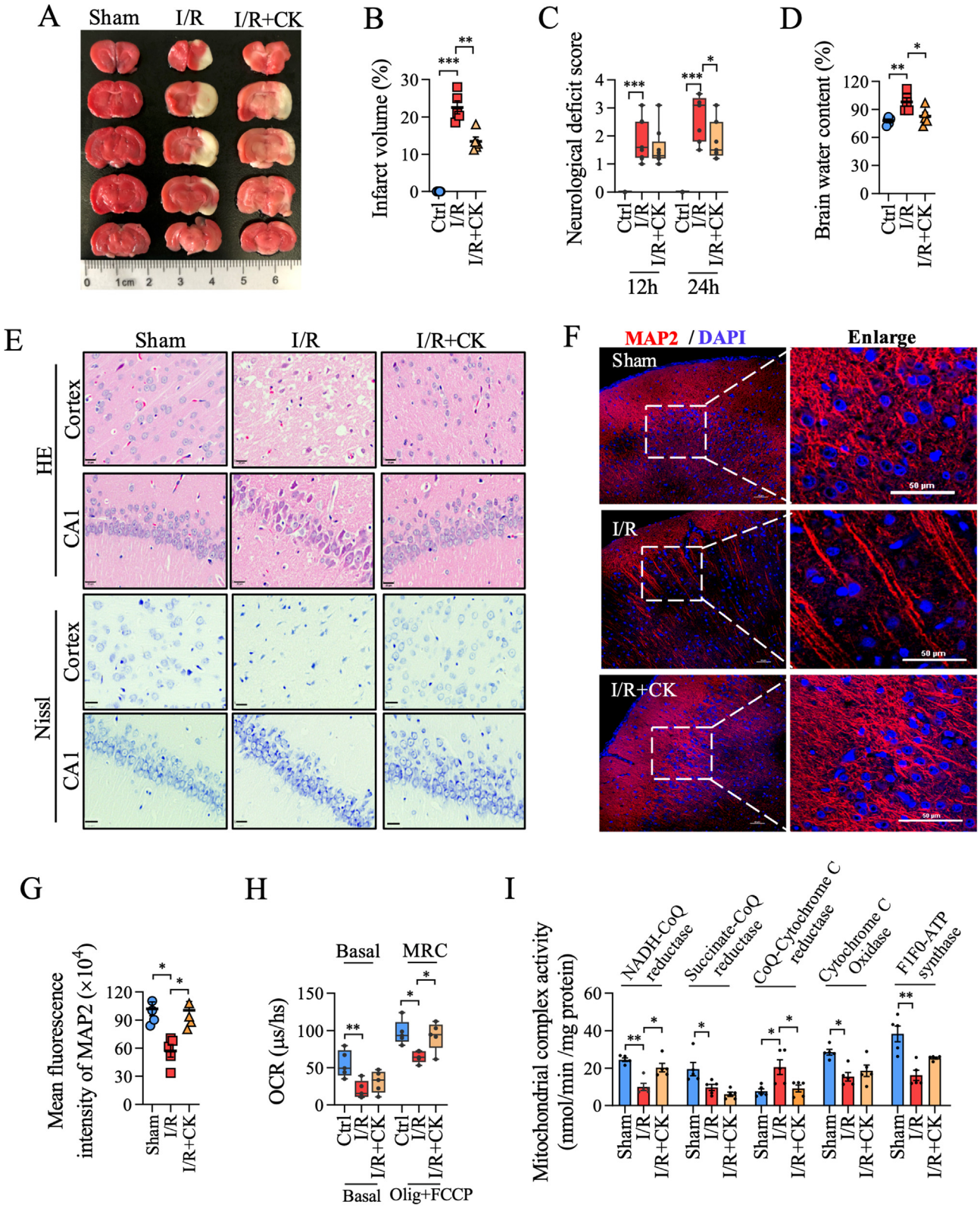

Fig. 4. Ginsenoside CK reduces neuronal injury and mitochondrial damage in the I/R rat model. (A) After ginsenoside CK pretreatment (10 mg/kg/day, 500 μL, dissolved in ddH_2O) for 14 days prior to I/R injury, TTC staining was used to detect the ischemic area in rat brain tissues from the sham group (without insert the nylon monofilament), I/R group (middle cerebral artery occlusion), and I/R + CK group; the red represents the living neurons, and the white represents the damaged neurons. **(B)** The ischemic volume in rat brain tissues from (A) was analyzed by ImageJ software. **(C)** Longa neurological deficiency scale was used to analyze the neurological function of rats. **(D)** The water content of brain tissue was measured by dry and wet weight method. **(E)** H&E and Nissl staining were used to analyze the degree of neuronal damage; scale bar = 20 μm. **(F)** The expression of MAP2 in cerebral cortex was detected by immunofluorescence assay; DAPI was used for staining nuclei; scale bar = 50 μm. **(G)** Quantitative analysis of the mean fluorescence intensity of MAP2 from (F). **(H)** Live mitochondria from cerebral cortical neurons of different groups were extracted to measure OCR in basal respiration and under the mitochondrial stress with

Detection of a neuron marker MAP2 by immunofluorescence staining also verified the neuroprotective effect of ginsenoside CK pretreatment (Fig. 4F and G). To further confirm the inhibitory effect of ginsenoside CK on I/R-induced mitochondrial dysfunction, we extracted mitochondria from fresh brain tissues to determine oxygen consumption and mitochondrial complex enzyme activity. As shown in Fig. 4H and I, ginsenoside CK pretreatment significantly restored the reductions in maximal respiration capacity (no effect on basal respiration) and the activities of complex I and III induced by I/R. Similar to *in vitro* experiments, ginsenoside CK had no effect on the protein expression of the mitochondrial complex in the I/R-injured rat model (Fig. S4C–Fig. S4D). Taken together, these results verified the effect of ginsenoside CK on the inhibition of neuronal damage and bioenergy imbalance in the *in vivo* I/R model.

3.5. Ginsenoside CK reduces mitochondrial fission and mitophagy in the rat I/R model

We further verified the regulatory role of ginsenoside CK in mitochondrial dynamics and mitophagy in the rat I/R model. First, we observed the ultrastructure of mitochondria through TEM and analyzed the mitochondrial aspect ratio, the number of mitochondria and autophagosomes. As shown in Fig. 5A, ginsenoside CK pretreatment significantly reduced mitochondrial division and autophagy, and slightly increased the mitochondrial account, compared with the I/R model group. Moreover, we observed the expressions of LC3, Parkin, and TOM20 in the different areas of brain tissue using a laser confocal microscope, and performed the co-localization analysis. In the CA1 region, the increase in LC3 expression after I/R incubation was significantly offset by ginsenoside CK pretreatment, while this phenomenon was not observed in the CA3 region (Fig. 5B and Fig. S5A–Fig. S5C). Interestingly, we found that ginsenoside CK pretreatment significantly inhibited the increase of Parkin–TOM20 co-localization induced by I/R in all regions of rat brain tissues, including cortex, gyrus, CA1, and CA3 regions (Fig. 5C and D). Taken together, these *in vivo* results demonstrate that ginsenoside CK administration significantly reduces I/R-induced mitochondrial fission and mitophagy in brain tissue.

3.6. Ginsenoside CK inhibits the ubiquitination of Mfn2 and the translocation of DRP1 by regulating Mul1 in the I/ R rat model

By immunoblot analyses, we found that ginsenoside CK pretreatment significantly abolished I/R-induced increased Mul1 expression, DRP1 translocation, and reduced Mfn2 expression, especially in mitochondria, which was similar with the results of our *in vitro* experiments (Fig. 6A and Fig. S6A). Confocal imaging further revealed that the reduction in Mfn2 expression induced by I/R was inhibited by ginsenoside CK pretreatment in the cortex and CA1 regions (Fig. 6B and Fig. S6B–S6C). Importantly, ginsenoside CK pretreatment augmented Mfn2 expression, accompanied by a significant reduction in ubiquitinated protein expression after I/R processing (Fig. 6C and Fig. S6D). To verify whether ginsenoside CK pretreatment directly reduces the effect of Mul1-mediated ubiquitination of Mfn2, we analyzed the interaction of Mul1 and Mfn2 by a co-IP experiment. Indeed, after Mul1 was immunoprecipitated, ginsenoside CK significantly blunted the binding of Mul1 to Mfn2 in cortex tissues during I/R (Fig. 6D). Similarly, the binding of Mfn2 to Mul1 was also inhibited by ginsenoside CK pretreatment, when Mfn2 was immunoprecipitated. Importantly, the ubiquitination of Mfn2 was significantly inhibited in the CK group, compared with the I/R group (Fig. 6D). Collectively, these data confirm that ginsenoside CK pretreatment reduces the binding affinity of Mul1 and Mfn2 to inhibit the ubiquitination and degradation of Mfn2, thereby elevating the protein level of Mfn2 and attenuating mitochondrial translocation of DRP1 against I/R injury.

4. Discussion

As postmitotic and high-energy-demanding cells, neurons are inevitably more prone to mitochondrial pathology [26]. Mitochondria undertake fusion and fission processes all the time for maintaining the balance of bioenergetic efficiency and energy expenditure, which is involved in the pathogenesis of cerebral I/R injury [27,28]. Mitochondrial fusion is a multistep and conserved process that begins with the mitofusins proteins-mediated juxtaposition and tethering of adjacent mitochondria, followed by conformational changes of mitofusins oligomers driven by GTP hydrolysis [29]. Mechanically, tethering and fusion for the outer mitochondrial membrane are mainly regulated by Mfn1, Mfn2, and homologous proteins that contain a GTPase domain (DRP1) [30]. Indeed, we observed that the phenotype of I/R-induced changes in mitochondrial morphology was accompanied by a significant reduction in the expression of Mfn1, Mfn2, and OPA1, and an elevation in mitochondrial Mul1, DRP1 and FIS1 expression. Importantly, we only observed significant changes in Mul1 and Mfn2 levels and DRP1 translocation upon manipulation of ginsenoside CK administration, which led us to consider that the Mul1-mediated Mfn2 and DRP1 expression could drive the effect of ginsenoside CK against I/R injury. Multiple studies have reported that Mul1 retards mitochondrial fusion through the ubiquitination and degradation of Mfn2 in the C-terminal RING finger domain, which is involved in the imbalance of mitochondrial dynamics, mitophagy, and bioenergy during metabolism stress [13]. Using a co-IP experiment, we found that ginsenoside CK pretreatment significantly inhibited the binding of Mul1 to Mfn2 to mediate Mfn2 degradation, thereby promoting the expansion and fusion of healthy mitochondria and further preventing mitochondrial dysfunction in response to I/R and OGD/R damage. Our findings provided new insights into the potential targets during I/R injury and the new molecular mechanism of ginsenoside CK, which are associated with mitochondrial dynamics and bioenergy.

Mitochondrial fragmentation–induced mitophagy and apoptosis are almost always observed during cerebral I/R injury, and DRP1 has therefore been mechanistically implicated in programmed cell apoptosis [31,32]. Emerging evidence suggests that DRP1 stimulates Bax oligomerization and Cyto C release by promoting mitochondrial fission and mitophagy, which are widely recognized as a culprit of neuronal injury, even programmed cell death [33,34]. However, in some studies, genetic or chemical overexpression of DRP1, accompanied by strengthened mitophagy and decreased Cyto C release, has shown a critical neuroprotective response against neuronal I/R injury [35]. Thus, there is an ongoing debate about the pros and cons of inhibiting fragmentation-induced mitophagy during cerebral I/R injury [33]. In this respect, we observed that I/R- or OGD/R incubation caused the changes in mitochondrial morphology, bioenergy imbalance, and neuronal injury, which are all accompanied by the translocation of DRP1 to mitochondria. Importantly, these phenotypes above were significantly reversed by ginsenoside CK pretreatment in the cell and animal models. In addition, the targeted inhibition of DRP1 by Mdivi-1 completely abolished the restraining effect of ginsenoside CK on I/R-induced mitophagy and mito-ROS burst but did not

oligomycin and FCCP. **(I)** Enzyme activity of the mitochondrial complexes in rat brain tissues was examined by enzymatic kits. Data are shown as mean ± SEM, n = 5 per group; *P < 0.05, **P < 0.01, ***P < 0.001, significantly different as indicated; one-way ANOVA followed by Tukey's post hoc test.

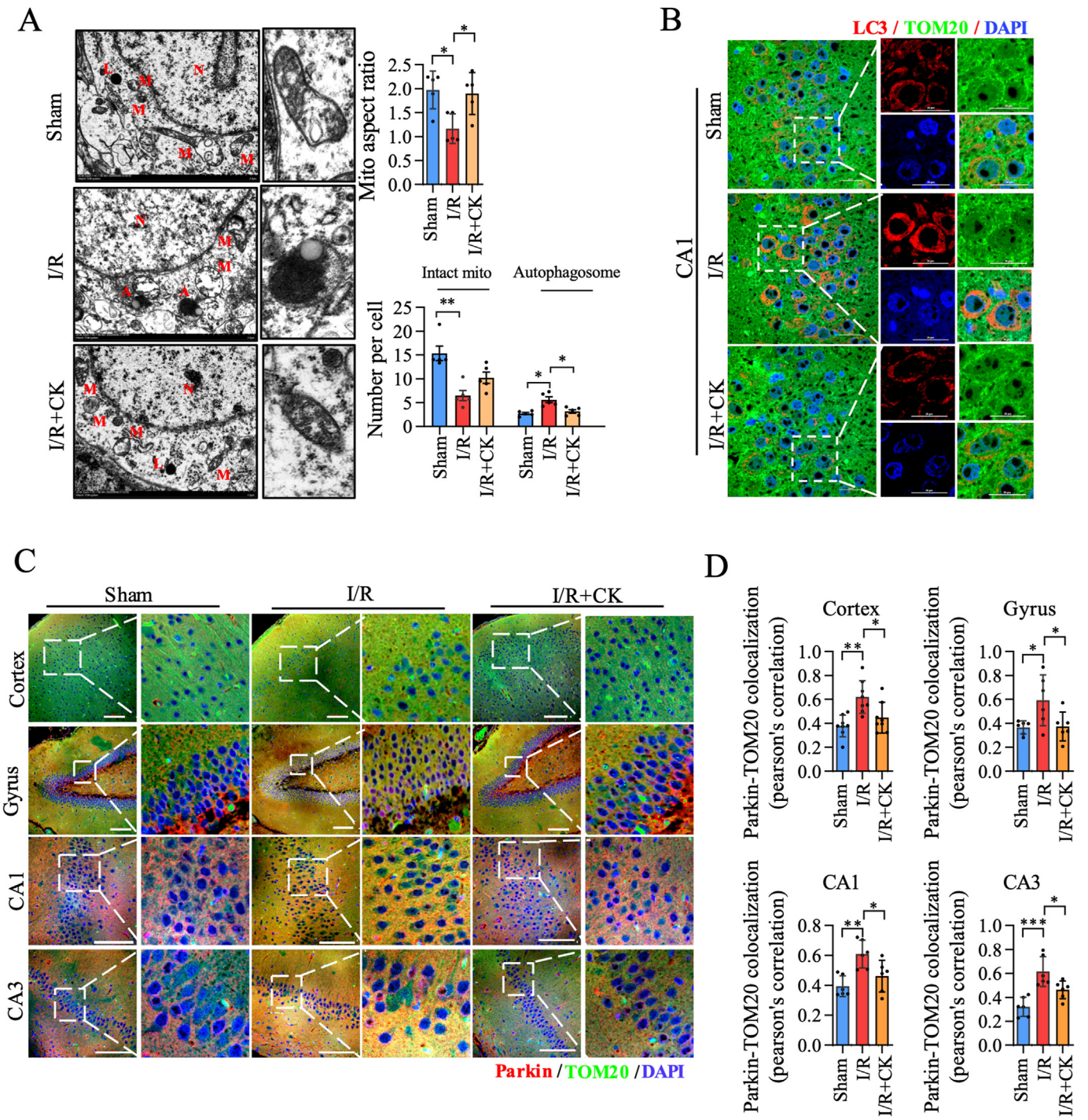

Fig. 5. Ginsenoside CK reduces mitochondrial fragmentation and mitophagy in the I/R model. (A) The ultrastructural morphology of mitochondria in rat brain tissues was examined by transmission electron microscopy. A: autophagosome; L: lysosome; M: mitochondria; N: nucleus. The aspect ratio of mitochondria and the number of mitochondrial autophagosomes were statistically analyzed and are shown on the right; scale bar = 1 μm. **(B)** The expression and localization of LC3 and TOM20 in neurons were detected by immunofluorescence assay; scale bar = 20 μm. **(C)** The expression and localization of Parkin and TOM20 in neurons of different regions were detected by immunofluorescence assay. Scale bar = 100 μm. **(D)** The co-localization of Parkin and TOM20 from (C) was quantitatively analyzed. Data are shown as mean ± SEM, n = 5 per group; *P < 0.05 and **P < 0.01, significantly different as indicated (one-way ANOVA followed by Tukey's post hoc test).

abrogate the interaction of Mul1 with Mfn2, which indicated that ginsenoside CK pretreatment inhibited the Mul1-regulated ubiquitination of Mfn2 to abolish DRP1-mediated fission, mitophagy, and apoptosis.

Ginsenoside CK is a secondary ginsenoside biotransformed from major ginsenosides, such as Rb1, Rb2, or Rc. Previous reports have shown that ginsenoside CK significantly inhibits I/R-induced rat neurological damage and OGD/R-induced neuronal autophagy and apoptosis [15,18]. Furthermore, ginsenoside CK administration can regulate multiple signaling pathways related to energy metabolisms, such as PI3K and AMPK in OGD/R-induced injury models [15,36]. Ginsenoside Rc, a metabolic precursor of ginsenoside CK,

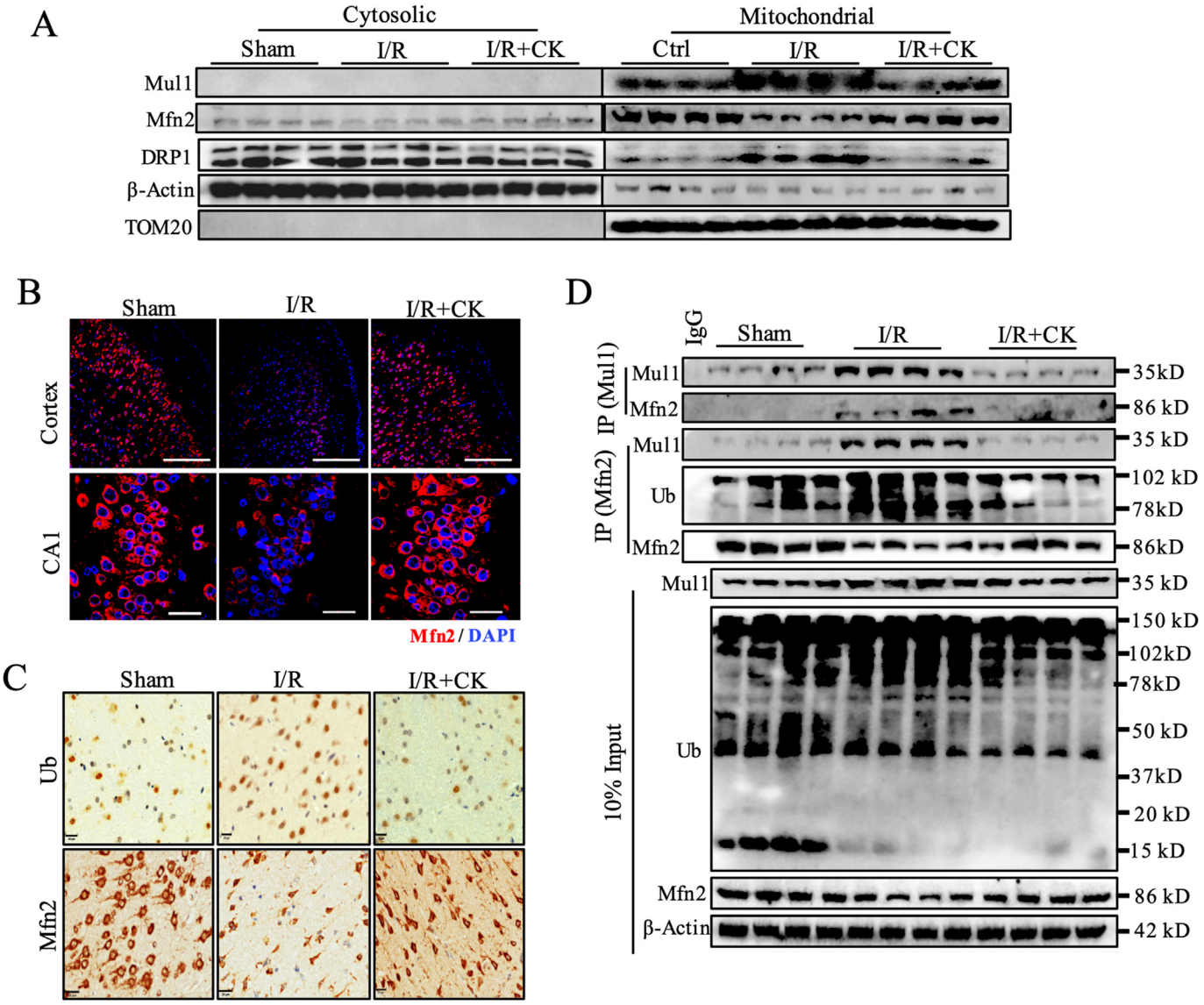

Fig. 6. Ginsenoside CK inhibits the activity of Mul1 and ubiquitination of Mfn2 in the I/ R rat model. (A) The protein expressions of Mul1, Mfn2 and DRP1 in the cytoplasm or mitochondria in rat brain tissues were detected by western blot. **(B)** The expression of Mfn2 protein in cortex (scale bar = 200 μm) and CA1 region (scale bar = 20 μm) was detected by immunofluorescence assay. **(C)** The expression of ubiquitin-protein and Mfn2 protein in brain tissues were detected by immunohistochemical staining; scale bar = 20 μm. **(D)** After the immunoprecipitation of Mul1 or Mfn2 antibody, the binding of Mul1 and Mfn2 and Mfn2 ubiquitination in fresh brain tissues were analyzed by co-IP and Western blot. Ub: ubiquitination, n = 5 per group.

can significantly restore the imbalance of neuronal energy metabolism and mitochondrial dysfunction induced by OGD/R or I/R injury [20]. Inspired by this interaction, we speculated that ginsenoside CK could regulate mitochondrial dynamics and bioenergy, thereby protecting neurons from cerebral I/R injury. Therefore, when we studied the mechanism of I/R damage based on mitochondrial dynamics and bioenergetics, we carried out the screening for different ginsenoside monomers. We expectedly found a typical dose-dependent effect of ginsenoside CK on mitochondrial aspect ratio, ATP level, and OCR in the OGD/R-induced neuronal injury model. More importantly, ginsenoside CK pretreatment inhibited the expression of Mul1 to regulate Mfn2 ubiquitination, mitochondrial dynamics and bioenergy, which contributed to the maintenance of mitochondrial integrity and neuroprotective properties in *in vivo* I/R and *in vitro* OGD/R models. These results provide a new mechanism for the beneficial effects of ginsenoside CK as natural preventive agent against cerebral I/R injury.

Of note, this study still had some limitations. First, mito-ROS was produced from complex I and complex III in cerebral I/R injury. In this study, total mito-ROS production was determined using MitoSOX™ dye, which was not able to distinguish the ROS from complex I or complex III. Particularly, accumulating evidence has suggested that ROS produced by complex I causes the neuronal deleterious effects, whereas ROS produced by complex III had the neuroprotective effects in mice with cerebral I/R injury [37]. Future studies are needed to determine how ginsenoside CK regulates ROS production by complex I or complex III to explain the potential function of ginsenoside CK in the reduction of mito-ROS production and mitochondrial depolarization. Second, previous studies have shown that patients with ischemic stroke or transient ischemic attack were characterized by significantly increased concentration of platelets and circulating platelet-leukocyte aggregate in blood [38,39]. Noteworthily, Jiahong Han. et al demonstrated ginsenoside CK (5mg/kg and 10 mg/kg) treatment significantly increased the

levels of platelet and red blood cells, while inhibited the percentage of leukocyte in mice induced by cyclophosphamide [40]. An increase in platelets may increase the risk of stroke, so further studies are needed to clarify the effect of different doses and times of ginsenoside CK on blood platelets. Finally, more robust data should be provided to substantiate these findings for a protective effect of ginsenoside CK against cerebral injury using Mul1 loss-of-function animal models.

5. Conclusion

In conclusion, ginsenoside CK pretreatment could attenuate mitochondrial translocation of DRP1, mitophagy, mitochondrial apoptosis, and neuronal bioenergy imbalance against cerebral I/R injury in both *in vitro* and *in vivo* models. Our data also confirmed that ginsenoside CK administration could reduce the binding affinity of Mul1 and Mfn2 to inhibit the ubiquitination and degradation of Mfn2, thereby elevating the protein level of Mfn2. Our findings provided new insights into the potential targets during I/R injury and the new molecular mechanism of ginsenoside CK, which are associated with mitochondrial dynamics and bioenergy. These data provide evidence that ginsenoside CK may be a promising therapeutic agent against cerebral I/R injury via Mul1/Mfn2–mediated mitochondrial dynamics and bioenergy.

Declaration of competing interest

The authors have no conflicts of interest to declare.

Acknowledgments

This work was supported by the National Natural Science Foundation of China, China (Grant No. 82104432 and U19A2013), the National Key Research and Development Program of China, China (Grant No. 2019YFC1709902), the Science and Technology Development Plan Project of Jilin Province, China (Grant No. YDZJ202201ZYTS270, 202002053JC and 20200201419JC), and the Jilin Provincial Administration of Traditional Chinese Medicine, China (Grant No. 20222222). We thank LetPub (www.letpub.com) for its linguistic assistance during the preparation of this manuscript.

Appendix A. Supplementary data

Supplementary data to this article can be found online at https://doi.org/10.1016/j.jgr.2022.10.004.

References

[1] Han J, Li Q, Ma Z, Fan J. Effects and mechanisms of compound Chinese medicine and major ingredients on microcirculatory dysfunction and organ injury induced by ischemia/reperfusion. Pharmacology & Therapeutics 2017;177:146–73.
[2] Liu F, Lu J, Manaenko A, Tang J, Hu Q. Mitochondria in ischemic stroke: new insight and implications. Aging and Disease 2018;9:924–37.
[3] Kumar R, Bukowski M, Wider J, Reynolds C, Calo L, Lepore B, et al. Mitochondrial dynamics following global cerebral ischemia. Mol Cell Neurosci. 2016;76:68–75.
[4] Gao S, Hu J. Mitochondrial fusion: the machineries in and out. Trends in Cell Biology 2021;31:62–74.
[5] Ten V, Galkin A. Mechanism of mitochondrial complex I damage in brain ischemia/reperfusion injury. A Hypothesis. Mol Cell Neurosci. 2019;100:103408.
[6] Chipuk J, Mohammed J, Gelles J, Chen Y. Mechanistic connections between mitochondrial biology and regulated cell death. Developmental Cell 2021;56:1221–33.
[7] Chen X, Wang Q, Shao M, Ma L, Guo D, Wu Y, et al. Ginsenoside Rb3 regulates energy metabolism and apoptosis in cardiomyocytes via activating PPARalpha pathway. Biomed Pharmacother 2019;120:109487.
[8] Liu Q, Dong Q. NR4A2 exacerbates cerebral ischemic brain injury via modulating microRNA-652/mul1 pathway. Neuropsychiatric Disease and Treatment 2020;16:2285–96.
[9] Burté F, Carelli V, Chinnery P, Yu-Wai-Man P. Disturbed mitochondrial dynamics and neurodegenerative disorders. Nature Reviews Neurology 2015;11:11–24.
[10] Schmitt K, Grimm A, Dallmann R, Oettinghaus B, Restelli L, Witzig M, et al. Circadian control of DRP1 activity regulates mitochondrial dynamics and bioenergetics. Cell Metabol. 2018;27:657–66. e5.
[11] Igarashi R, Yamashita S, Yamashita T, Inoue K, Fukuda T, Fukuchi T, et al. Gemcitabine induces Parkin-independent mitophagy through mitochondrial-resident E3 ligase MUL1-mediated stabilization of PINK1. Sci Rep. 2020;10:1465.
[12] Yuan Y, Li X, Xu Y, Zhao H, Su Z, Lai D, et al. Mitochondrial E3 ubiquitin ligase 1 promotes autophagy flux to suppress the development of clear cell renal cell carcinomas. Cancer Sci. 2019;110:3533–42.
[13] Puri R, Cheng X, Lin M, Huang N, Sheng Z. Defending stressed mitochondria: uncovering the role of MUL1 in suppressing neuronal mitophagy. Autophagy 2020;16:176–8.
[14] Sharma A, Lee H. Ginsenoside compound K: insights into recent studies on pharmacokinetics and health-promoting activities. Biomolecules 2020;10.
[15] Huang Q, Lou T, Wang M, Xue L, Lu J, Zhang H, et al. Compound K inhibits autophagy-mediated apoptosis induced by oxygen and glucose deprivation/reperfusion via regulating AMPK-mTOR pathway in neurons. Life Sci. 2020;254:117793.
[16] Oh J, Jeong J, Park S, Chun S. Ginsenoside compound K induces adult hippocampal proliferation and survival of newly generated cells in young and elderly mice. Biomolecules 2020;10.
[17] Oh J, Kim J. Compound K derived from ginseng: neuroprotection and cognitive improvement. Food & Function 2016;7:4506–15.
[18] Park J, Shin J, Jung J, Hyun J, Van Le T, Kim D, et al. Anti-inflammatory mechanism of compound K in activated microglia and its neuroprotective effect on experimental stroke in mice. J Pharmacol Exp Therapeut. 2012;341:59–67.
[19] Qi H, Zhang Z, Liu J, Chen Z, Huang Q, Li J, et al. Comparisons of isolation methods, structural features, and bioactivities of the polysaccharides from three common panax species: a review of recent progress. Molecules. 2021;26.
[20] Huang Q, Su H, Qi B, Wang Y, Yan K, Wang X, et al. A SIRT1 activator, ginsenoside rc, promotes energy metabolism in cardiomyocytes and neurons. J Am Chem Soc. 2021;143:1416–27.
[21] Cheng CQ, Wan Y, Yang W, Tian M, Wang Y, He H, et al. Gastrodin protects H9c2 cardiomyocytes against oxidative injury by ameliorating imbalanced mitochondrial dynamics and mitochondrial dysfunction. Acta Pharmacol Sin 2020;41:1314–27.
[22] Zhang Q, Wang Z, Miao L, Wang Y, Chang L, Guo W, et al. Neuroprotective effect of SCM-198 through stabilizing endothelial cell function. Oxid Med Cell Longev 2019;2019:7850154.
[23] Geng J, Liu W, Gao J, Jiang C, Fan T, Sun Y, et al. Andrographolide alleviates Parkinsonism in MPTP-PD mice via targeting mitochondrial fission mediated by dynamin-related protein 1. Br J Pharmacol 2019;176:4574–91.
[24] Lilley E, Stanford S, Kendall D, Alexander S, Cirino G, Docherty J, et al. ARRIVE 2.0 and the British journal of pharmacology: updated guidance for 2020. Br J Pharmacol 2020;177:3611–6.
[25] Raimundo L, Paterna A, Calheiros J, Ribeiro J, Cardoso D, Piga I, et al. BBIT20 inhibits homologous DNA repair with disruption of the BRCA1-BARD1 interaction in breast and ovarian cancer. Br J Pharmacol. 2021;178:3627–47.
[26] Iwata R, Casimir P, Vanderhaeghen P. Mitochondrial dynamics in postmitotic cells regulate neurogenesis. Science (New York, NY) 2020;369:858–62.
[27] Carinci M, Vezzani B, Patergnani S, Ludewig P, Lessmann K, Magnus T, et al. Different roles of mitochondria in cell death and inflammation: focusing on mitochondrial quality control in ischemic stroke and reperfusion. Biomedicines 2021;9.
[28] Zhao H, Pan W, Chen L, Luo Y, Xu R. Nur77 promotes cerebral ischemia-reperfusion injury via activating INF2-mediated mitochondrial fragmentation. Journal of Molecular Histology 2018;49:599–613.
[29] Pernas L, Scorrano L. Mito-morphosis: mitochondrial fusion, fission, and cristae remodeling as key mediators of cellular function. Annual Review of Physiology 2016;78:505–31.
[30] Ma R, Ma L, Weng W, Wang Y, Liu H, Guo R, et al. DUSP6 SUMOylation protects cells from oxidative damage via direct regulation of Drp1 dephosphorylation. Sci Adv 2020;6. eaaz0361.
[31] Anzell A, Maizy R, Przyklenk K, Sanderson T. Mitochondrial quality control and disease: insights into ischemia-reperfusion injury. Molecular Neurobiology 2018;55:2547–64.
[32] Zuo W, Yang P, Chen J, Zhang Z, Chen N. Drp-1, a potential therapeutic target for brain ischaemic stroke. British Journal of Pharmacology 2016;173:1665–77.
[33] Yang J, Mukda S, Chen S. Diverse roles of mitochondria in ischemic stroke. Redox Biology 2018;16:263–75.
[34] Yin Y, Sun G, Li E, Kiselyov K, Sun D. ER stress and impaired autophagy flux in neuronal degeneration and brain injury. Ageing Research Reviews 2017;34:3–14.

[35] Chen W, Sun Y, Liu K, Sun X. Autophagy: a double-edged sword for neuronal survival after cerebral ischemia. Neural Regeneration Research 2014;9:1210–6.
[36] Li X, Huang Q, Wang M, Yan X, Song X, Ma R, et al. Compound K inhibits autophagy-mediated apoptosis through activation of the PI3K-akt signaling pathway thus protecting against ischemia/reperfusion injury. Cell Physiol Biochem: Int J Exp Cell Physiol Biochem Pharmacol 2018;47:2589–601.
[37] Chouchani E, Pell V, James A, Work L, Saeb-Parsy K, Frezza C, et al. A unifying mechanism for mitochondrial superoxide production during ischemia-reperfusion injury. Cell Metabol 2016;23:254–63.
[38] Ishikawa T, Shimizu M, Kohara S, Takizawa S, Kitagawa Y, Takagi S. Appearance of WBC-platelet complex in acute ischemic stroke, predominantly in atherothrombotic infarction. Journal of Atherosclerosis and Thrombosis 2012;19:494–501.
[39] Bladowski M, Gawrys J, Gajecki D, Szahidewicz-Krupska E, Sawicz-Bladowska A, Doroszko A. Role of the platelets and nitric oxide biotransformation in ischemic stroke: a translative review from bench to bedside. Oxidative Medicine and Cellular Longevity 2020;2020:2979260.
[40] Han J, Wang Y, Cai E, Zhang L, Zhao Y, Sun N, et al. Study of the effects and mechanisms of ginsenoside compound K on myelosuppression. J Agric Food Chem 2019;67:1402–8.